

Research Article

Integration Analysis of MicroRNA and mRNA Expression Profiles in Human Peripheral Blood Lymphocytes Cultured in Modeled Microgravity

C. Girardi,¹ C. De Pittà,¹ S. Casara,¹ E. Calura,¹ C. Romualdi,¹ L. Celotti,^{1,2} and M. Mognato¹

¹ Dipartimento di Biologia, Università degli Studi di Padova, Via U. Bassi 58/B, 35131 Padova, Italy

² Laboratori Nazionali di Legnaro, INFN, Viale dell'Università 2, Legnaro, 35020 Padova, Italy

Correspondence should be addressed to L. Celotti; luca.celotti@unipd.it and M. Mognato; maddalena.mognato@unipd.it

Received 16 April 2014; Revised 22 May 2014; Accepted 22 May 2014; Published 23 June 2014

Academic Editor: Mariano Bizzarri

Copyright © 2014 C. Girardi et al. This is an open access article distributed under the Creative Commons Attribution License, which permits unrestricted use, distribution, and reproduction in any medium, provided the original work is properly cited.

We analyzed miRNA and mRNA expression profiles in human peripheral blood lymphocytes (PBLs) incubated in microgravity condition, simulated by a ground-based rotating wall vessel (RWV) bioreactor. Our results show that 42 miRNAs were differentially expressed in MMG-incubated PBLs compared with 1 g incubated ones. Among these, miR-9-5p, miR-9-3p, miR-155-5p, miR-150-3p, and miR-378-3p were the most dysregulated. To improve the detection of functional miRNA-mRNA pairs, we performed gene expression profiles on the same samples assayed for miRNA profiling and we integrated miRNA and mRNA expression data. The functional classification of miRNA-correlated genes evidenced significant enrichment in the biological processes of immune/inflammatory response, signal transduction, regulation of response to stress, regulation of programmed cell death, and regulation of cell proliferation. We identified the correlation of miR-9-3p, miR-155-5p, miR-150-3p, and miR-378-3p expression with that of genes involved in immune/inflammatory response (e.g., IFNG and IL17F), apoptosis (e.g., PDCD4 and PTEN), and cell proliferation (e.g., NKX3-1 and GADD45A). Experimental assays of cell viability and apoptosis induction validated the results obtained by bioinformatics analyses demonstrating that in human PBLs the exposure to reduced gravitational force increases the frequency of apoptosis and decreases cell proliferation.

1. Introduction

Exposure to spaceflight environment is known to cause in humans many adverse physiological changes, including skeletal muscle atrophy [1–3], cardiovascular and microvascular disorders [4–6], bone deterioration [7, 8], and impaired immune system function [9, 10]. Immune system dysfunction due to exposure to microgravity has been documented as well in terms of reduced activation/proliferation, altered cytokine production, and altered signal transduction [11, 12]. Alterations in global gene expression patterns have been also observed in space-flown human cells, involving mainly genes of immune system activation [13, 14], cytoskeleton [15], and cell cycle [16, 17]. However, due to the difficulty and limitations of performing experiments in the real microgravity of space, many investigations have been conducted under simulated microgravity conditions, in which cells are

cultured in ground-based machines, such as clinostats and rotating wall vessel bioreactors that generate a residual 10^{-3} – 10^{-6} g force that approximates microgravity [5, 18–24]. The results indicate that, similar to space microgravity, simulated microgravity affects both cell structure and function, as well as gene expression, in mammalian cells [14, 19, 25], in bacteria [26, 27], or in other living organisms [28–30].

Since molecular changes at the gene level may compromise cell function, it is important to understand the cellular response to reduced gravity at the molecular level. For this purpose, a class of noncoding RNAs, called microRNAs (miRNAs), plays a key role. miRNAs are a large family of small RNAs of 18–24 nucleotides that are involved in post-transcriptional regulation of gene expression by interacting with 3'-untranslated regions (UTR) of target genes. The regulatory process is complex and occurs posttranscriptionally through miRNA interaction with a target site in the mRNA

that has partial or complete complementarity to the miRNA. The binding of miRNAs to complementary sequence of their target mRNAs may repress translation or induce degradation of mRNAs [31]. Recently, the destabilization of target mRNAs, instead of translational repression, has been shown to be the predominant mechanism for reduced protein output [32]. Less often, dsRNA formed by miRNA target complexes can target gene promoters and actually enhance transcription of target genes, sometimes termed RNAa (RNA activation) [33]. A single miRNA may have broad effects on gene expression networks, such as regulating cell lineage specificity, cellular functions, or stress response. Besides a physiological role of miRNAs in a variety of important biological processes including differentiation, apoptosis [34], and fat metabolism [35], the miRNA-mediated gene regulation operates also during viral infection [36], stress response pathway [37], and pathological processes, such as tumorigenesis [38–42].

The present study is addressed to identify alterations in miRNA profiles of human peripheral blood lymphocytes (PBLs) incubated in modeled microgravity (MMG) with respect to those incubated in gravity 1g. To simulate microgravity, we used a specialized bioreactor developed at the NASA-Johnson Space Center (Houston, TX, USA), the rotating wall vessel, which represents a valid ground model to simulate, as far as possible, a condition of reduced gravity. To identify miRNA-correlated genes whose expression level was significantly altered as a function of MMG, we performed gene expression profiling on the same PBL samples assayed for miRNA profiling and we integrated microRNAome and transcriptome by using MAGIA² [43], a web tool for the integrative analysis of miRNA and genes expression data incorporating transcriptional regulation. A group of miRNA-mRNA pairs related to immunity, cell proliferation, and apoptosis was identified in PBLs incubated in MMG. The differences between MMG and 1g on correlated miRNA-mRNA pairs involved in cell proliferation and apoptosis were investigated by *in vitro* assays of clonogenic ability and apoptosis induction in PBLs incubated in MMG with respect to those incubated in 1g conditions.

2. Materials and Methods

2.1. Lymphocytes Isolation and Microgravity Simulation. Human peripheral blood lymphocytes (PBLs) were obtained from freshly collected “buffy coats” from blood samples of twelve healthy anonymous donors at the Blood Centre of the City Hospital of Padova (Italy). This study obtained the Ethics Approval from the Transfusion Medicine (TM) Ethics Committee of Blood Centre of the City Hospital of Padova. PBLs were isolated by separation on Biocoll density gradient (BIOCHROM, Berlin, Germany). After isolation, PBLs were preincubated overnight at a concentration of 3×10^6 /mL in basal medium RPMI 1640 containing GlutaMAX I (Invitrogen Life Technologies, Carlsbad, CA, USA), 124 U/mL penicillin, 63 μ g/mL streptomycin sulfate, and 10% fetal bovine serum (FBS, BIOCHROM, Berlin, Germany). After the overnight incubation, PBLs, consisting of peripheral mononuclear cells depleted of monocytes, were suspended

at 1×10^6 /mL in basal medium and subjected to modeled microgravity, simulated by the rotating wall vessel (RWV) bioreactor (Synthecon, Cellon), placed inside a humidified incubator, vertically rotating at 23 rpm [44]. In the rotating system, the gravity is balanced by equal and opposite mechanical forces (centrifugal, Coriolis, and shear components), and the gravitational vector is reduced to about 10^{-3} g. In these conditions, single cells are nearly always in suspension, rotating in quasi-stationary manner with the fluid, in a low-shear culture environment [19, 45]. Ground-based (1g) PBLs were kept at the same cell density in 75 cm² flasks (FALCON) in the same medium. After 24, 48, or 72 h of incubation in MMG and 1g PBLs were activated to enter cell cycle to measure cell proliferation by incubation in culture medium (CM) containing phytohaemagglutinin (PHA, BIOCHROM, Berlin, Germany) and interleukin 2 (IL2, Chiron Siena, Italy) as stimulating factors [46].

2.2. Total RNA Isolation. Total RNA was isolated from 10^7 PBLs at the end of 24 h incubation in MMG and 1g by using Trizol Reagent (Invitrogen Life Technologies, Carlsbad, CA, USA), according to the manufacturer’s protocol. Total RNA was quantified using the ND-1000 spectrophotometer (Nanodrop, Wilmington, DE, USA) and RNA integrity and the content of miRNAs were assessed by capillary electrophoresis using the Agilent Bioanalyzer 2100, as previously described [47]. Only total RNA samples with RNA integrity number (RIN) values ≥ 6 and with miRNA $< 20\%$ were used for microarray analysis.

2.3. miRNA and Gene Expression Profiling. MicroRNAs profiling was carried out in PBL samples incubated in MMG versus 1g. Analyses were performed by using the “Human miRNA Microarray kit (V2)” (Agilent Technologies) that allows the detection of 723 known human (miRBase v.10.1) and 76 human viral miRNAs. Total RNA (200 ng) was labeled with pCp Cy3, according to the Agilent protocol and unincorporated dyes were removed with MicroBioSpin6 columns (BioRad) [48]. Probes hybridization and slides washing were performed as previously reported [47]. Agilent Feature Extraction software version 10.5.1.1 was used for image analysis.

Gene expression profiling was carried out in MMG-incubated PBLs versus 1g incubated PBLs on total RNA extracted from the same PBL samples assayed for miRNA profiling. We used the “Whole Human Genome Oligo Microarray” (Agilent), consisting of $\sim 41,000$ (60-mer) oligonucleotide probes, which span conserved exons across the transcripts of the targeted full-length genes. 800 ng of total RNA was labeled with “Agilent One-Color Microarray-Based Gene Expression protocol” according to the manufacturer’s instructions. The method uses T7 RNA polymerase, which simultaneously amplifies target material and incorporates cyanine 3-labeled CTP. The Cy3-labeled cRNAs were purified using Qiagen’s RNeasy mini spin columns (Qiagen) and quantified using the ND-1000 spectrophotometer (Nanodrop, Wilmington, DE, USA). Probes hybridization and slides washing were performed as previously reported [47].

Slides were scanned on an Agilent Microarray Scanner System (model G2565CA) and Agilent Feature Extraction software version 10.5.1.1 was used for image analysis. Raw data are available on the Gene Expression Omnibus (GEO) website (<http://www.ncbi.nlm.nih.gov/geo/>) using SuperSeries accession number GSE57418 that groups microRNA (GSE57400) and mRNA expression profiles (GSE57408).

2.4. Statistical Analysis of miRNA and Gene Expression Data. Interarray normalization of expression levels was performed with cyclic Lowess for miRNA experiments and with quantile for gene expression profiling [49] to correct possible experimental distortions. Normalization function was applied to expression data of all experiments and then values of spot replicates within arrays were averaged. The modalities of spot quality measures and hybridization are reported previously [47]. The identification of differentially expressed genes and miRNAs was performed with one- and two-class Significance Analysis of Microarray (SAM) program [50] with default settings. The expression level of each miRNA and mRNA was calculated as the \log_2 (MMG/1g) PBLs of the same donor. Pathway analysis on differentially expressed genes has been performed using Graphite web [51], hypergeometric test on Reactome Pathways, considering significant those categories with $FDR < 0.1$.

2.5. Identification of miRNA Target Genes and Correlation Analysis of miRNA and mRNA Expression Data. To predict miRNA targets, we performed a computational analysis integrating mRNA and miRNA expression measurements from the same donor using MAGIA² web tool [43], freely available at <http://gencomp.bio.unipd.it/magia2/>. We used <http://www.microrna.org/> predictions and Pearson correlation ($r > 0.4$) to estimate the degree of correlation between any putative pairs of miRNA and mRNA [52, 53]. To identify the biological processes most involved in target prediction, we have performed an enrichment analysis on Gene Ontology (GO) using DAVID web tool v6.7 [54] considering significant those categories with $FDR < 0.2$.

Intraclass analyses have been performed considering MMG and 1g samples separately. In order to have comparable results, the intraclass analysis has been performed using MAGIA² software with the same parameters, predictors, and cutoff described for the previous analysis. Specific interactions for MMG and 1g networks have been identified and a GO enrichment analysis ($FDR < 0.2$) was performed separately on the nodes belonging to the specific MMG and 1g networks using DAVID web tool.

2.6. Quantitative Real-Time PCR (qRT-PCR) Assay. In order to verify the expression data generated by miRNA and mRNA microarrays, we performed qRT-PCR experiments for miRNAs and genes which showed significant expression changes in MMG. The following miRNAs were subjected to the RT-qPCR validation: miR-9-5p, miR-378a, miR-155-5p, and miR-150-3p. Reverse transcription of 10 ng of total RNA with primers corresponding to each miRNA and to U48 small nuclear RNA (RNU48) as endogenous control

was performed as directed by the protocol of the two-step TaqMan MicroRNA Assay kit (Applied Biosystems, Foster City, CA, USA) that incorporates a target-specific stem-loop reverse transcription primer to provide specificity for the mature miRNA target. For the PCR reaction, 1 μ L of the RT reaction was combined with 0.5 μ L of TaqMan MicroRNA Assay 20x and 5 μ L of TaqMan Universal PCR Master Mix in a 10 μ L final volume. The reactions were incubated in a Mastercycler EP gradient S (Eppendorf) in 0.2 mL PCR tubes for 30 min at 16°C and 30 min at 42°C, followed by 5 min at 85°C, and then held at 4°C. The resulting cDNA was quantitatively amplified in 40 cycles on an ABI 7500 Real-Time PCR System, using TaqMan Universal PCR Master Mix and TaqMan MicroRNA Assays.

For mRNA detection, 1 μ g of total RNA was retro-transcribed with ImProm-II Reverse Transcription System (Promega). qRT-PCR was performed with the GoTaq qPCR Master Mix (Promega) and gene-specific primers for IFNG, IL17F, TLR4, HLA-DRB1, and BCL6 genes and for GAPDH as reference. qRT-PCR reactions were performed in quadruplicates, in PBL samples from 6 to 8 donors. Real-time PCR was performed using an Applied Biosystems 7500 Fast Real-Time PCR System with cycling conditions of 95°C for 10 min followed by 95°C for 15 sec and 60°C for 60 sec, 45 cycles in total. The relative expression levels of miRNAs and mRNAs between samples were calculated using the comparative delta CT (threshold cycle number) method ($2^{-\Delta\Delta CT}$) implemented in the 7500 Real-Time PCR System software [55]. Primers' pairs used are as follows: GAPDH (glyceraldehyde-3-phosphate dehydrogenase): fw 5'-TCC-TCTGACTTCAACAGCGA-3'; rev 5'-GGGTCTTACTCC-TTGGAGGC-3'; IFNG (interferon gamma): fw 5'-GGC-ATTTTGAAGAATTGGAAAG-3'; rev 5'-TTTGGATGC-TCTGGTCATCTT-3'; IL17F (interleukin 17): fw 5'-GGC-ATCATCAATGAAAACCA-3'; rev 5'-TGGGGTCCCAAG-TGACAG-3'; TLR4 (Toll-like receptor 4): fw 5'-CCTGCG-TGAGACCAGAAAAG-3'; rev 5'-TTCAGCTCCATGCAT-TGATAA-3'; HLA-DRB1 (major histocompatibility complex, class II, DR beta 1): fw 5'-ACAACACTACGGGGTTG-TGGAG-3'; rev 5'-GCTGCCTGGATAGAAACCAC-3'; BCL6 (B-cell CLL/lymphoma 6): fw 5'-CGAATCCACACA-GGAGAGAAA-3'; rev 5'-ACGCGGTATTGCACCTTG-3'.

2.7. Cell Proliferation and Apoptosis Induction. Cell viability was determined by the T-cell cloning assay [44, 46] at the end of 24 h, 48 h, and 72 h incubation in MMG and 1g. Briefly, four 96-well U-bottomed microtiter plates with two viable lymphocytes/well were seeded in medium CM in the presence of 1×10^4 feeder cells/well (TK6 lymphoblastoid cells lethally irradiated with 40 Gy of γ -rays). Two weeks later, the plates were scored for growing colonies to calculate the cloning efficiency (CE) from the proportion of negative wells assuming a Poisson distribution ($CE = -\ln P_0/N$, where P_0 is the fraction of wells without cells and N is the number of cells seeded into wells) [56].

Apoptotic index was determined in PBLs incubated for 24 and 48 h in MMG and in parallel in 1g. For detection of apoptotic morphology, PBLs were fixed and stained with

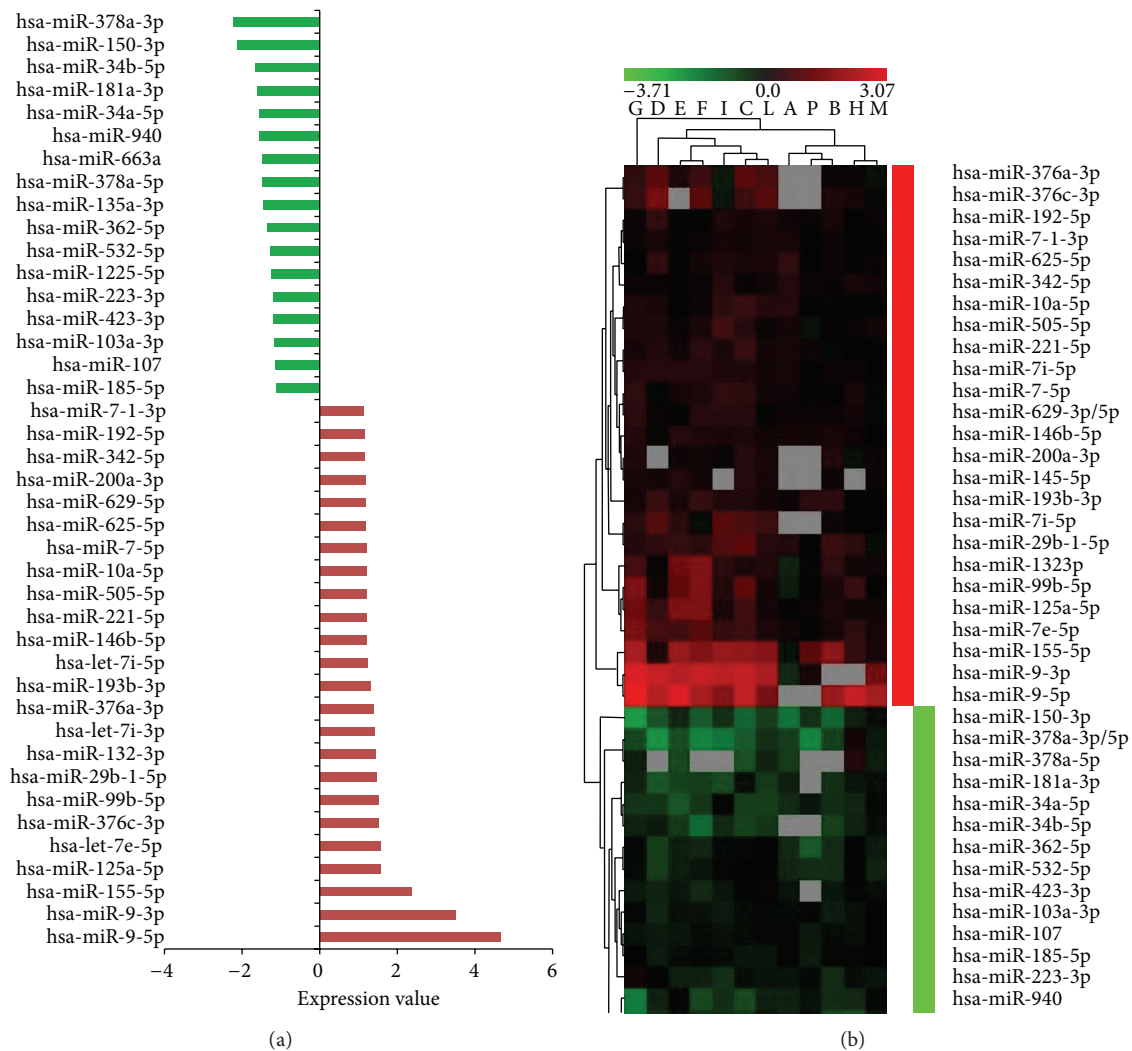


FIGURE 1: Differentially expressed miRNAs in human PBLs incubated in MMG. (a) The expression level of each miRNA, indicated as fold change, is the mean of the expression values obtained from the transformed log₂ ratio (MMG/1 g). (b) Dendrogram of miRNAs differentially expressed in MMG. The range of expression value is from -3.7 (green, downregulation) to 3.07 (red, upregulation). Grey boxes correspond to not available (N/A) fluorescent signal from the microarray platform.

2 $\mu\text{g}/\text{mL}$ 4,6-diamino-2-phenylindol (DAPI, Roche), in an antifade solution (Vectashield, Vector Lab) as previously described [57]. At least 2000 cells were scored for each time-point by fluorescence microscopy (1000x magnification). The activation of caspase-3 was measured by the caspase-3 fluorescent assay kit (Clontech BD Biosciences) at the end of incubation in 1 g or MMG, as previously described [58]. The fluorescent emission at 505 nm (excitation at 400 nm) of cleaved 7-amino-4-trifluoromethyl coumarin (AFC) was measured with a PerkinElmer LS-50 B spectrofluorimeter.

3. Results

3.1. Identification of miRNAs Affected by Microgravity. miRNA expression profiling was performed on total RNA extracted from PBLs of twelve healthy donors at the end of

24 h incubation time in MMG and in 1 g conditions. By comparing the expression profile of MMG-incubated versus 1 g incubated PBLs of the same donor, we found 42 differentially expressed miRNAs, 25 upregulated and 17 downregulated, for which raw data and means of miRNA expression values are available at Supplementary Table S1 (see Supplementary Table S1 in the Supplementary Material available online at <http://dx.doi.org/10.1155/2014/296747>). miR-9-5p, miR-9-3p, and miR-155-5p were the most upregulated (4.6-, 3.5-, and 2.4-fold, resp.), whereas miR-378a and miR-150-3p were the most downregulated (~2-fold) (Figure 1).

3.2. Effect of Microgravity on Gene Expression Profile. Gene expression analysis was performed in PBLs incubated for 24 h in MMG and in 1 g. By comparing the expression profiles of MMG-incubated and 1 g incubated PBLs, we identified 1581 differentially expressed genes in MMG versus 1 g, among

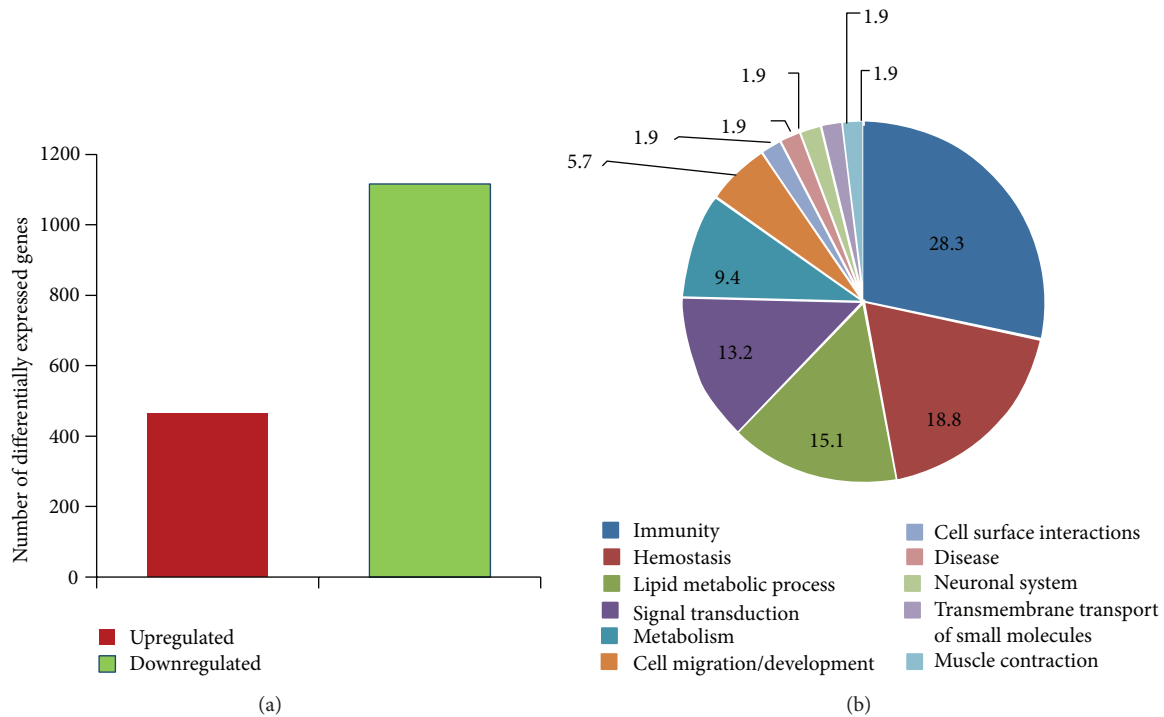


FIGURE 2: Results of gene expression analysis. Differentially expressed genes (a) and pie chart of biological process (%) containing pathways significantly enriched in PBLs incubated in MMG (b).

which 465 (29%) genes were upregulated whereas 1116 (71%) genes were downregulated (Figure 2(a) and Supplementary Table S2). By selecting a 2-fold cut-off threshold, we identified 312 (19.7%) genes in MMG; 157 genes (10%) showed alterations in expression level with a fold change greater than 4.0, and, among these, 20 genes showed a fold change ≥ 16.0 (Supplementary Table S3). To identify sets of genes with expression changes in MMG condition, we used Graphite [51], a novel web tool for topological-based pathway analyses based on high-throughput gene expression data analyses. Pathway analysis on differentially expressed genes has been performed by using hypergeometric test on Reactome Pathways as implemented in Graphite web, considering significant those categories with $FDR < 0.1$. We evidenced biological pathways significantly enriched in MMG: 15 (28.3%) were related to immunity, 10 (18.8%) to hemostasis, 7 (13.2%) to lipid metabolic process and signal transduction, 5 (9.4%) to metabolism, 3 (5.7%) to cell migration/development, and 1 (1.9%) to cell surface interactions, disease, neuronal system, transmembrane transport of small molecules, and muscle contraction (Figure 2(b)). The list of pathways is reported in Supplementary Table S4.

Among the immune pathways significantly enriched in MMG, those of “MHC class II antigen presentation,” “Toll Receptor Cascades,” and “DAPI2 signaling” showed the highest number of differentially expressed genes (30, 20, and 20 genes, resp.). Also the “interferon gamma signaling” pathway was significantly enriched in MMG, with 13 differentially expressed genes. Ten genes codifying for proteins of MHC class II (HLA-DRA, HLA-DRB1, HLA-DRB3, HLA-DRB4,

HLA-DRB5, HLA-DQA1, HLA-DQA2, HLA-DPA1, HLA-DPBI, and HLA-DQB1) were common to nine pathways (Figure 3). CD4, codifying for a membrane glycoprotein of T lymphocytes that interacts with the major histocompatibility complex class II antigens, was common to eight immune pathways; RELA, PTEN, and PAK1 were included in three pathways, whereas HLA-DOA and HLA-DMB were included in two pathways.

3.3. Target Prediction and Integration Analysis of miRNA and mRNA Expression Profiles. We examined the regulatory effects of miRNAs on global gene expression under modeled microgravity (MMG) condition in comparison with ground gravity (1g). To predict the target genes of differentially expressed miRNAs in MMG, we performed a computational analysis using TargetScan tool, which predicts biological targets of miRNAs by searching for the presence of conserved 8 mer and 7 mer sites that match the seed region of each miRNA [59]. However, all available software for target prediction is characterized by a large fraction of false positive; thus, the integration of target predictions with miRNA and gene target expression profiles has been proposed to refine miRNA-mRNA interactions. The correlation analyses on the differentially expressed miRNAs and mRNAs were carried out with MAGIA² software [43], by microRNA Pearson prediction analysis, which allowed the identification of miRNA-mRNA interactions (Supplementary Table S5). To discover functional relationships between miRNAs and the transcriptome and uncover the gene pathways that are regulated

Gene symbol description		Fold change	Interferon gamma signaling	PD-1 signaling	Phosphorylation of CD3 γ and TCR zeta chains	Translocation of ZAP-70 to immunological synapse	Generation of second messenger molecules	MHC class II antigen presentation	Downstream TCR signaling	TCR signaling	Costimulation by the CD28 family	DAP12 signaling	Toll receptor cascade
<i>HLA-DPA1</i>	Major histocompatibility complex, class II, DP alpha 1	-1.78	■	■	■	■	■	■	■	■	■	■	■
<i>HLA-DPB1</i>	Major histocompatibility complex, class II, DP beta 1	-1.83	■	■	■	■	■	■	■	■	■	■	■
<i>HLA-DQA1</i>	Major histocompatibility complex, class II, DQ alpha 1	-1.51	■	■	■	■	■	■	■	■	■	■	■
<i>HLA-DQA2</i>	Major histocompatibility complex, class II, DQ alpha 2	-1.64	■	■	■	■	■	■	■	■	■	■	■
<i>HLA-DQB1</i>	Major histocompatibility complex, class II, DQ beta 1	-1.4	■	■	■	■	■	■	■	■	■	■	■
<i>HLA-DRA</i>	Major histocompatibility complex, class II, DR alpha	-1.55	■	■	■	■	■	■	■	■	■	■	■
<i>HLA-DRB1</i>	Major histocompatibility complex, class II, DR beta 1	-1.61	■	■	■	■	■	■	■	■	■	■	■
<i>HLA-DRB3</i>	Major histocompatibility complex, class II, DR beta 3	-1.85	■	■	■	■	■	■	■	■	■	■	■
<i>HLA-DRB4</i>	Major histocompatibility complex, class II, DR beta 4	-1.74	■	■	■	■	■	■	■	■	■	■	■
<i>HLA-DRB5</i>	Major histocompatibility complex, class II, DR beta 5	-1.59	■	■	■	■	■	■	■	■	■	■	■
<i>HLA-DOA</i>	Major histocompatibility complex, class II, DO alpha	-0.95	■	■	■	■	■	■	■	■	■	■	■
<i>HLA-DMB</i>	Major histocompatibility complex, class II, DM beta	-1.47	■	■	■	■	■	■	■	■	■	■	■
<i>CD4</i>	CD4 molecule	-0.78	■	■	■	■	■	■	■	■	■	■	■
<i>RELA</i>	v-rel reticuloendotheliosis viral oncogene homolog A	0.51	■	■	■	■	■	■	■	■	■	■	■
<i>PTEN</i>	Phosphatase and tensin homolog	-0.26	■	■	■	■	■	■	■	■	■	■	■
<i>PAK1</i>	p21 protein (Cdc42/Rac)-activated kinase 1	-1.32	■	■	■	■	■	■	■	■	■	■	■

FIGURE 3: Differentially expressed genes common to immune-related pathways identified by Reactome database in PBLs incubated in MMG. The expression value of each gene, indicated as fold change, is the mean of expression levels calculated as the log₂ ratio (MMG/1g) on PBL samples (see Supplementary Table S2).

by miRNAs in MMG, we performed Gene Ontology (GO) analysis using DAVID [54].

In our analysis, we used high classification stringency and considered only GO terms that have $P < 0.1$ after permutation corrections (Benjamini) (Table 1). Several GO terms belonged to immune system function (i.e., “innate immune response,” “inflammatory response,” “regulation of cytokine production,” “positive regulation of immune system process,” and “response to bacterium”), in accordance with the results of pathway analysis on transcriptome (see Supplementary Table S4). GO terms of “cell development,” “regulation of cell differentiation,” “regulation of cell communication,” “cell motility,” and “cell migration” were significantly enriched in MMG, together with the category “organ development.” In addition, the biological categories of “regulation of signal transduction,” “regulation of response to stress,” “regulation of cell death,” and “regulation of cell proliferation” were enriched in PBLs incubated in MMG.

To determine whether different miRNAs within a GO category interact with the same target genes, we performed network analysis using MAGIA² [43], a software platform for the visualization of complex miRNA-mRNA interactions. We focused on miRNAs that correlated both positively and negatively with the GO categories of immune/inflammatory

response, regulation of programmed cell death, and regulation of cell proliferation. As shown in Figure 4, most transcripts are associated with more than one miRNA, as in the case of TLR4 transcript, correlated with eight different miRNAs (miR-10a-5p, miR-7-5p, miR-135a-3p, miR-103a-3p, miR-7-1-3p, miR-107, miR-629-5p, and miR-362-5p).

By using Cytoscape [60], we visualized the functional interactions between miRNAs whose expression levels changed the most in PBLs incubated in MMG, such as miR-9-5p, miR-9-3p, miR-155-5p, miR-150-3p, and miR-378a-3p, and correlated target genes involved in GO categories of immune/inflammatory response, regulation of programmed cell death, and regulation of cell proliferation (Figure 5).

Our results show that miR-155-5p correlates with IFNG, IL17F, BCL6, and RELA involved in immune/inflammatory response, with PTEN, BNIP3L, APAF1, and PDCD4 involved in regulation of programmed cell death, and with NKX3-1 involved in regulation of cell proliferation; miR-150-3p correlates with immune-related genes (IFNG, IL1A, and HLA-DRB1) and with proapoptotic gene PDCD4; miR-9-3p correlates with genes regulating cell proliferation (NKX3-1, GADD45A, and TP53BP1), apoptosis (APAF1, BNIP3L), and immunity (CCL7, CXCL5, and BCL6). Among genes enriched within the three functional categories, miR-9-5p

TABLE 1: Selected GO terms of biological processes significantly affected by microgravity. The complete list of GO terms can be found in Supplementary Table S6.

GO:ID	Term	Count	P value	Fold enrichment	FDR
GO:0045087	Innate immune response	25	$2,42 \times 10^{-5}$	2,566978193	0,040412626
GO:0009966	Regulation of signal transduction	88	$1,67 \times 10^{-4}$	1,471577879	0,27973741
GO:0048468	Cell development	62	$1,71 \times 10^{-4}$	1,610338849	0,285253218
GO:0045595	Regulation of cell differentiation	54	$2,68 \times 10^{-4}$	1,648	0,448057857
GO:0006954	Inflammatory response	41	$3,23 \times 10^{-4}$	1,787513228	0,539044451
GO:0080134	Regulation of response to stress	37	$5,43 \times 10^{-4}$	1,806696296	0,90478009
GO:0010646	Regulation of cell communication	95	$8,22 \times 10^{-4}$	1,380599647	1,366092587
GO:0048513	Organ development	139	$8,22 \times 10^{-4}$	1,290910116	1,366713032
GO:0042060	Wound healing	26	$8,38 \times 10^{-4}$	2,025910165	1,393334889
GO:0007165	Signal transduction	198	0,001398603	1,211224944	2,313943814
GO:0001817	Regulation of cytokine production	27	0,001406003	1,926233766	2,326052387
GO:0048514	Blood vessel morphogenesis	26	0,001709187	1,93009009	2,820918727
GO:0001817	Regulation of cytokine production	15	0,001406003	1,926233766	2,326052387
GO:0007399	Nervous system development	88	0,002097026	1,359812471	3,450524099
GO:0022603	Regulation of anatomical structure morphogenesis	28	0,002408369	1,831111111	3,953172097
GO:0048870	Cell motility	33	0,002838826	1,710188679	4,64407324
GO:0048522	Positive regulation of cellular process	159	0,003551259	1,221594406	5,777298149
GO:0002684	Positive regulation of immune system process	31	0,003855111	1,711490787	6,256755641
GO:0050865	Regulation of cell activation	26	0,003880839	1,819447983	6,297247375
GO:0051174	Regulation of phosphorus metabolic process	51	0,003964604	1,486259947	6,428964883
GO:0001944	Vasculature development	28	0,003981783	1,767969349	6,455956993
GO:0043066	Negative regulation of apoptosis	41	0,004040803	1,56952381	6,548633436
GO:0010941	Regulation of cell death	83	0,004115909	1,341019608	6,666445839
GO:0009617	Response to bacterium	22	0,004991824	1,9032021	8,030143455
GO:0043067	Regulation of programmed cell death	82	0,00552374	1,328770895	8,849108723
GO:0008285	Negative regulation of cell proliferation	40	0,00576007	1,54741784	9,210770389
GO:0010557	Positive regulation of macromolecule biosynthetic process	62	0,006543793	1,39014966	10,4004889
GO:0016477	Cell migration	30	0,006706505	1,664646465	10,64564555
GO:0042127	Regulation of cell proliferation	71	0,009848433	1,331149033	15,2576907
GO:0048523	Negative regulation of cellular process	139	0,012514364	1,19870225	18,9945349

correlates with BCL6. miR-378a-3p is correlated with HLA-DRB1, GPNMB, and NKX3-1; the same transcripts, together with IL17F, are correlated also with miR-378a-5p.

The microarray data from miRNA and gene expression profiling were validated by real-time qPCR experiments for four miRNAs (miR-9-5p, miR-155-5p, miR-378a, and miR-150-3p) and five mRNAs (IFNG, IL17F, BCL6, HLA-DRB1, and TLR4) whose expression level was significantly altered by MMG incubation (Figure 6). miR-9-5p and miR-155-5p, together with IFNG, IL17F, and BCL6 transcripts, were upregulated in MMG, whereas miR-378a and miR-150-3p together with HLA-DRB1 and TLR4 transcripts were downregulated in MMG.

3.4. Intra-class Integrated Analysis. Recently, Censi and colleagues [61] observed a significant increase in the number and strength of genes correlation under stress conditions, such as disease and environmental or physiological changes. To evaluate whether the stress induced by MMG increases the amount of correlation of the system with respect to

1g control condition, we integrated mRNAs and miRNAs data separately for MMG and 1g using MAGIA². By comparing the two regulatory networks, we observed a similar number of interactions between MMG (190 interactions) and 1g (218 interactions) (Figure S1), indicating that there was no significant connectivity enrichment under modeled microgravity. By contrast, Gene Ontology analysis performed on MMG- and 1g-specific interactions reported 50 GO categories significantly enriched in only MMG condition ($P < 0.2$ after Benjamini corrections, Supplementary Table S7); 10 out of these were previously described in Table 1. In particular, the GO categories “regulation of cellular process” and “cell differentiation” were significantly affected by MMG. With intraclass analysis, the GO categories of immunity and cell death were not enriched in MMG probably because, in our study, the number of PBL samples available for such analysis was relatively small. On the whole, the intraclass analysis shows that modeled microgravity does not increase the general connectivity of miRNA-gene interaction network but rather increases the transcriptome plasticity with respect

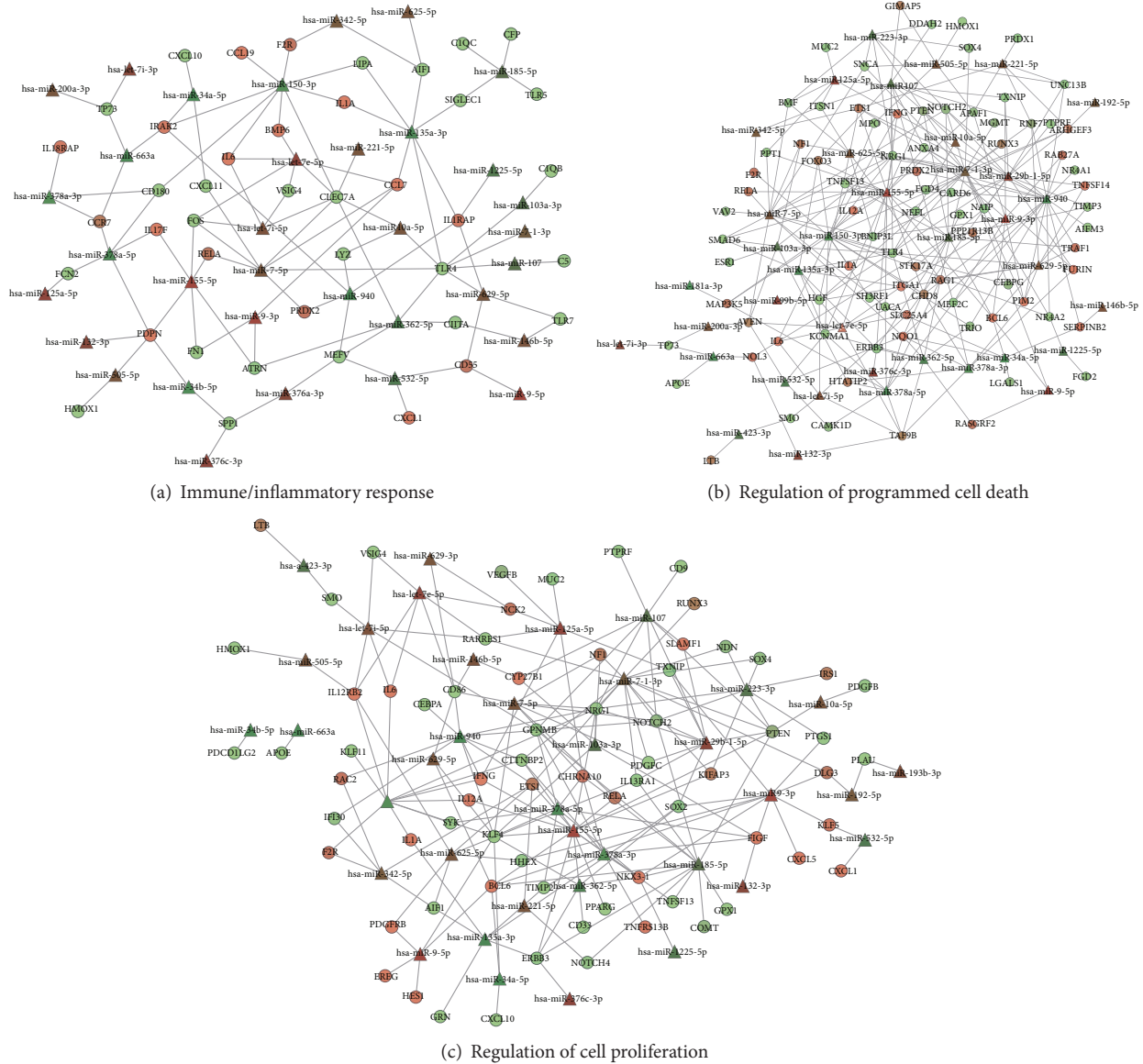


FIGURE 4: Network analysis on correlated miRNA-mRNA pairs in PBLs incubated in MMG. Network analyses were performed by MAGIA² software using miRNAs correlating both positively and negatively with transcripts involved in immune/inflammatory response (a), in regulation of programmed cell death (b), and in regulation of cell proliferation (c). Circles represent transcripts and triangles represent miRNAs.

to 1g gravity condition, as evidenced by the enriched GO categories.

3.5. In Vitro Validation of GO Analysis: Effects of MMG on Cell Proliferation and Apoptosis. Experimental assays were performed to validate the results obtained by bioinformatics analyses on the GO categories “regulation of cell proliferation” and “regulation of programmed cell death” associated with variations in miRNA expression under MMG. To measure cell proliferation, quiescent (G_0) PBLs from the same donor were incubated for different times (24 h, 48 h, and 72 h) in 1g and in MMG. At the end of incubation times, the colony

forming ability has been determined by the T-cell cloning assay [44], in which cells were incubated in medium containing mitogen factors (i.e., PHA and IL2) to trigger their cell cycle entry. Our results showed that cloning efficiency (CE) decreased with time in both gravity conditions; however, MMG incubation affected the ability of PBLs to form colonies ($P < 0.05$ at 24 h, Figure 7(a)). To investigate whether MMG incubation increased the frequency of apoptotic cells, PBLs were scored for the presence of apoptotic bodies. Apoptotic index was very similar at 24 and 48 h and significantly higher in PBLs incubated in MMG than in 1g (Figure 7(b), $P < 0.05$). In the same PBL samples, caspase-3 activation, assayed by the cleavage of the peptide substrate DEVD-AFC,

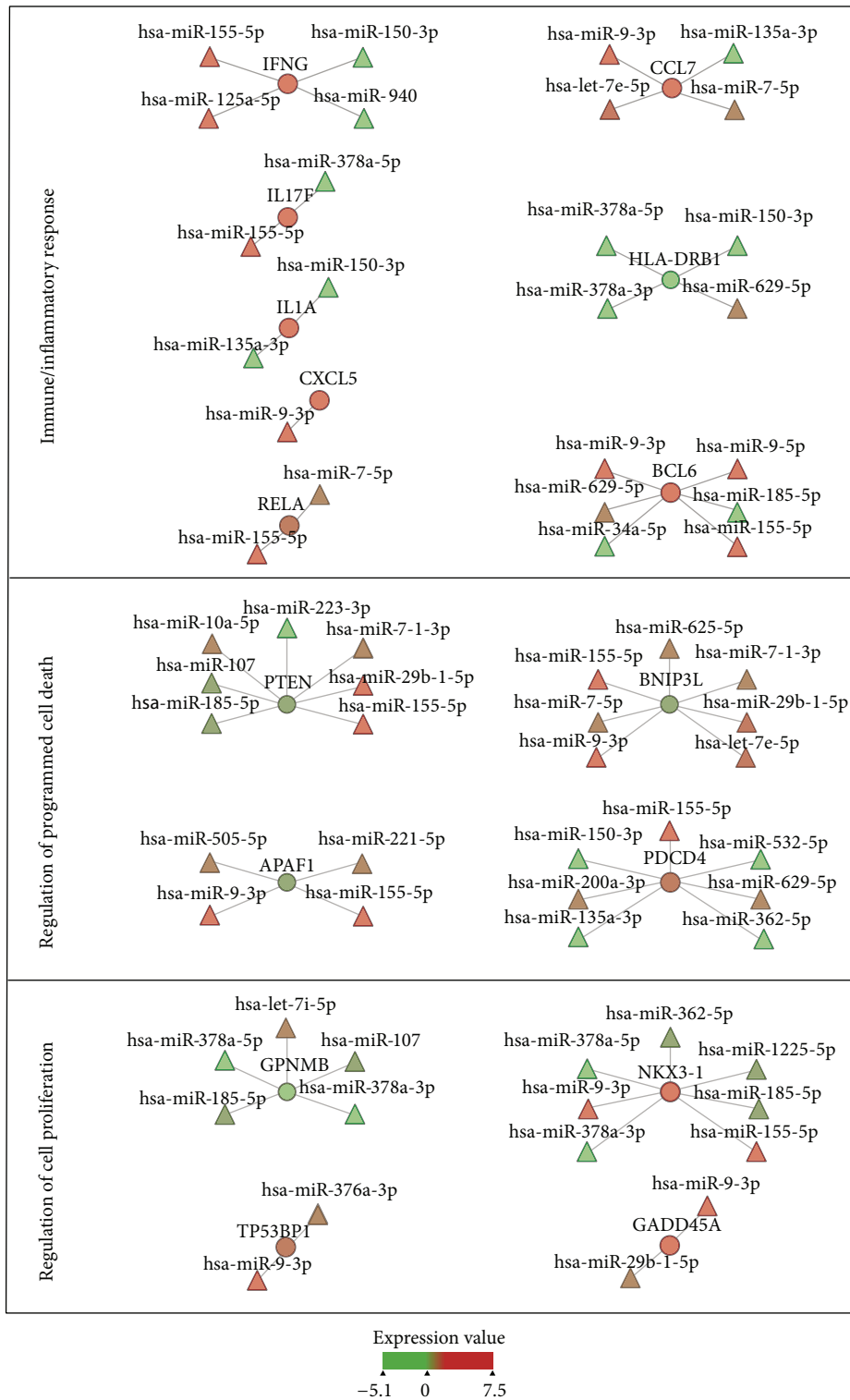


FIGURE 5: Cytoscape visualization of miRNA-mRNA correlations in PBLs incubated 24 h in MMG. Relationships between miRNAs and correlated target genes involved in “immune/inflammatory response” (IFNG, CCL7, IL17F, HLA-DRB1, IL1A, CXCL5, RELA, and BCL6), “regulation of programmed cell death” (PTEN, BNIP3L, APAF1, and PDCD4), and “regulation of cell proliferation” (GPNMB, NKX3-1, TP53BP1, and GADD45A). Circles represent transcripts and triangles represent miRNAs; the expression levels of each feature are represented as color scale.

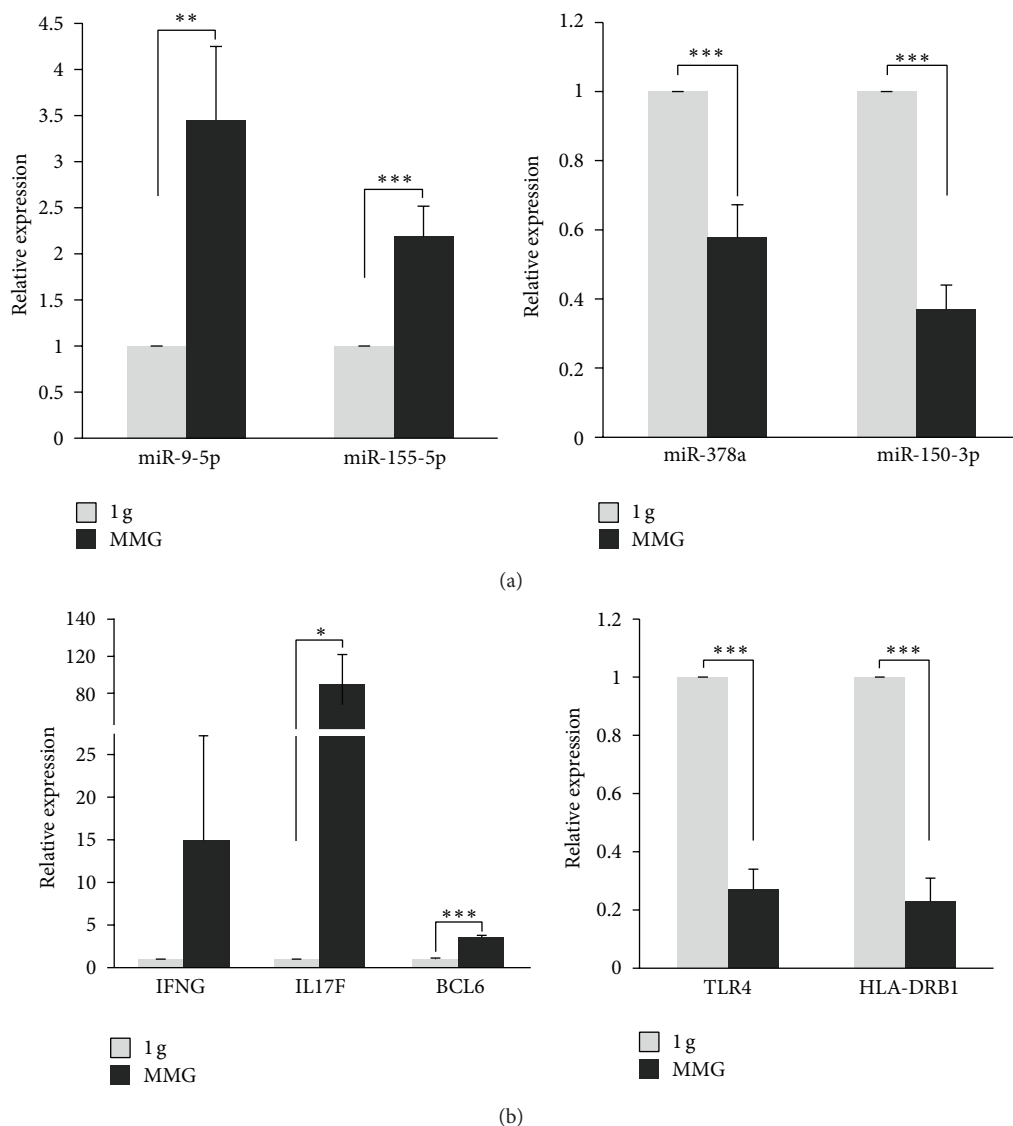


FIGURE 6: Microarray data validation by quantitative real-time PCR (qRT-PCR). Validation of microarray data by qRT-PCR in MMG-incubated versus 1g incubated PBLs. The results are consistent with the cumulative microarray data of miRNAs (a) and mRNAs (b). Values (fold change, dark grey bars) are means \pm S.E. of expression levels calculated as the \log_2 (MMG/1g) on PBL samples from 4 to 6 different donors. The value "1" of control 1g PBLs (light grey bars) is arbitrarily given when no change is observed (*** $P < 0.001$, ** $P < 0.01$, and * $P < 0.05$, t -test).

increased significantly in PBLs incubated 48 h in MMG with respect to those in 1g (Figure 7(c), $P < 0.05$).

4. Discussion

In the present study, we evaluated the effects of modeled microgravity (MMG) on human PBLs by analyzing miRNA and gene expression profiles in comparison with PBLs cultured in Earth gravity condition (1g). Our results reported 42 differentially expressed miRNAs in PBLs cultured for 24 h in MMG with respect to 1g, of which 14 (miR-34a-5p, miR-34b-5p, miR-663a, miR-135a-3p, miR-1225-5p, miR-940, miR-221-5p, miR-29b-1-5p, miR-10a-5p, let-7i-3p, miR-200a-3p, miR-7-5p, miR-7-1-3p, and miR-505-5p) were found altered also

by γ -irradiation, as assessed in our previous study [47]. The most dysregulated miRNAs identified in the present work are the upregulated miR-9-5p, miR-9-3p, and miR-155-5p, and the downregulated ones are miR-150-3p and miR-378a-3p. Such miRNAs have been found altered in human tumors; in particular, miR-9 is an oncogenic miRNA overexpressed in mixed lineage leukemia- (MLL-) rearranged acute myeloid leukemia [62], in muscle-invasive bladder cancer [63], and in osteosarcoma cell lines [64]. miR-155 is commonly upregulated in hematological malignancies [65, 66] and has been linked to the development of breast, lung, and stomach tumors [67–70]. miR-150 is significantly downregulated in most cases of acute myeloid leukemia [71] and colorectal cancer [72]; in addition, miR-150 has an important role in

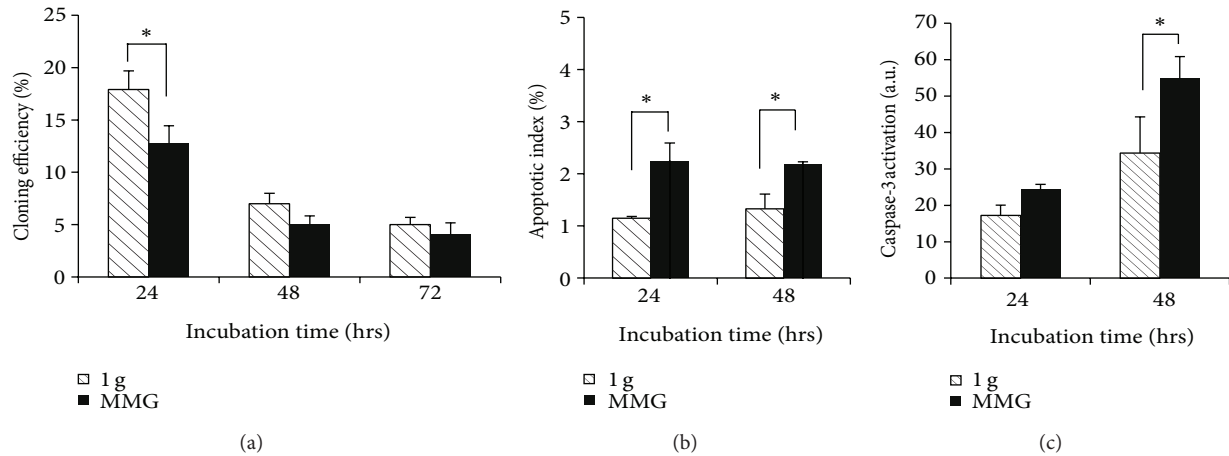


FIGURE 7: Cell proliferation and apoptosis induction in human PBLs incubated in MMG and in 1g. (a) T-cell cloning assay performed at the end of 24 h, 48 h, and 72 h of incubation in the two gravity conditions. Data are means \pm S.E. from thirteen independent experiments. (b) Apoptotic index at the end of incubation for 24 h and 48 h in MMG and 1g determined by nuclear chromatin condensation with DAPI staining. (c) Caspase-3 activation at the end of 24 h and 48 h incubation in MMG and 1g assessed by fluorimetric assay (a.u. arbitrary units). Data in (b) and (c) are means \pm S.E. from 3-4 independent experiments (* $P < 0.05$, t -test).

normal hematopoiesis and its aberrant downregulation is a sensitive marker indicative of lymphocyte depletion and bone marrow damage [73]. miR-378 (actually annotated as miR-378a) is significantly downregulated in colorectal cancer [74], in cutaneous squamous cell carcinoma [75], and in renal cell carcinoma [76]. The effects of microgravity on miRNA expression profile are currently reported in only one study carried out in human lymphoblastoid TK6 cells incubated under simulated microgravity for 72 h [77]. Among the dysregulated miRNAs, only two were common to our data, miR-150 and miR-34a, although the direction and intensity of fold change were different, demonstrating the cell type specific signature of miRNA profile.

miRNAs modulate gene expression by interacting with the 3'UTR of target genes, and since a single miRNA could have hundreds to thousands of predicted target genes [25], it is difficult to determine the true target regulated by the miRNA which affects a biological function. Moreover, binding of multiple miRNAs to one target could further increase the complexity of target prediction. The identification of miRNA target genes is usually performed by bioinformatic prediction algorithms based on (i) sequence similarity search, possibly considering target site evolutionary conservation, and (ii) thermodynamic stability. However, it is known that the results of target prediction algorithms are characterized by very low specificity [78]. For this purpose, the integration of target predictions with miRNA and gene expression profiles has been recently proposed to improve the detection of functional miRNA target relationships [79, 80]. Therefore, to identify the most likely target genes of miRNAs differentially expressed in MMG, we defined gene expression signature on the same samples of PBLs assayed for miRNA profiling; then, we integrated expression profiles from both miRNAs and mRNAs with *in silico* target predictions to reduce the number of false positives and increase the number of

biologically relevant targets [81–83]. Our results of gene expression profiling reported the downregulation of multiple genes in MMG (71%), in accordance with previous findings in activated human T lymphocytes incubated for 24 h in simulated microgravity [21]. Moreover, we found that about 20% of genes responded to MMG by more than 2-fold change in expression level and twenty genes showed a ≥ 16 -fold change in expression. Most of these top dysregulated genes were immune-related, such as those codifying for inflammatory cytokines (CCL1, CCL7, CXCL5, CXCL11, and IL1A) and for proteins with a role in immunoregulatory functions (IFNG, TNIP3, TREM1, APOC1, FCN1, FCN2, and CPVL) (Supplementary Table S3). Biological pathways enriched in PBLs exposed to MMG were mainly involved in immunity (Figure 2(b)), including adaptive immune system response (i.e., PD-1 signaling, phosphorylation of CD3 and TCR zeta chains, translocation of ZAP-70 to immunological synapse MHC class II antigen presentation, TCR signaling, and costimulation by the CD28 family), innate immune system response (i.e., Toll Receptor Cascades), and cytokine signaling in immune system (i.e., interferon gamma signaling) (Supplementary Table S4). All these pathways included ten downregulated genes codifying for MHC molecules class II (HLA-DPA1, HLA-DPB1, HLA-DQA1, HLA-DQA2, HLA-DQB1, HLA-DRA, HLA-DRB1, HLA-DRB3, HLA-DRB4, and HLA-DRB5), which are expressed in antigen presenting cells (APC) and play a central role in the immune system by presenting peptides derived from extracellular proteins [84]. Therefore, the downregulation of these genes suggests that the display of antigens at the cell surface of APC may be disturbed by gravity reduction, affecting the efficiency of immune response as observed in astronauts during spaceflight and immediately afterwards [85–87]. Moreover, our data are in accordance with the inhibition of immediate early genes in T-cell activation observed in space microgravity [14]

and with alterations of gene expression in human activated T-cells incubated in modeled microgravity, including the downregulation of HLA-DRA gene [21].

By integrating the transcriptome and microRNAome, we detected significant miRNA-mRNA relationships under MMG. Since miRNAs act prevalently through target degradation, expression profiles of miRNAs and target genes are generally expected to be inversely correlated. Nevertheless, since miRNA activity is part of complex regulatory networks and gene expression profiles are the result of different levels of regulation, also positive correlation (i.e., upregulated miRNA/upregulated mRNA or downregulated miRNA/downregulated mRNA) is expected. Indeed, in an *in vivo* mouse model, the activated expression of miRNAs has been shown to correlate with activated expression of mRNAs rather than with mRNA downregulation [88]. Gene Ontology (GO) analysis conducted on the significantly correlated miRNA-mRNA pairs evidenced the biological categories significantly overrepresented in MMG (Table 1). Many GO terms of immune response were enriched, such as “innate immune response,” “inflammatory response,” “regulation of cytokine production,” “positive regulation of immune system process,” and “response to bacterium.” Notably, the most dysregulated miRNAs detected in the present study, miR-378a-3p, miR-150-3p, miR-155-5p, miR-9-3p, and miR-9-5p, are significantly correlated with immune-related genes. In particular, miR-378a-3p is positively correlated with transcripts of MHC molecules class II such as HLA-DRB1 (Figure 5) and HLA-DOA, HLA-DRB5, and HLA-DQA2 (not shown). miR-150-3p is negatively correlated with HLA-DRB1, IFNG, and IL1A transcripts, whereas miR-155-5p is positively correlated with IFNG and IL17F and negatively correlated with RELA and BCL6 (Figure 5). IL1A, IL17F, and IFN- γ are proinflammatory cytokines acting during the immune response; IFN- γ is a soluble cytokine having broader roles in activation of immune responses, in part through upregulating transcription of genes involved in antigen processing/presentation, in cell cycle regulation and apoptosis, and its correlation with miR-155 has been recently validated [89]. BCL6, which encodes a nuclear transcriptional repressor, has a role not only in regulation of lymphocyte function, but also in cell survival and differentiation. Similarly, the pleiotropic transcription factor RELA has a role in immune biological process and it is also involved in cell growth and apoptosis. Besides miR-155-5p, BCL6 is correlated with four miRNAs including miR-9 (3p and 5p); in addition, miR-9-3p is positively correlated with CCL7 and CXCL5 (Figure 5). Recent evidences show that miR-9 is highly involved in immunity and inflammatory diseases [90–92] by enhancing IFN- γ production in activated human CD4(+) T-cells [91]. Moreover, Gao et al. [90] have shown that miR-9 disturbs the display of antigens at the cell surface by suppressing the expression of MHC class I gene transcription.

Together with the categories of immune response, GO analysis reported that also the categories of regulation of cell proliferation and regulation of programmed cell death were significantly enriched in MMG, as previously reported in γ -irradiated PBLs [47]. Interestingly, such categories were not enriched from pathway analysis conducted on transcriptome

and the reason could be that integrated analysis of miRNAs and mRNAs expression profiles evidences the posttranscriptional effect mediated by miRNAs on gene expression. Among genes involved in cell proliferation, the transcription factor NKX3-1 (2.4-fold upregulated), which mediates non-cell autonomous regulation of gene expression and inhibits cell proliferation, is correlated with miR-9-3p, miR-155-5p, miR-378a-3p, and miR-378-5p (Figure 5). TP53BP1 (1.4-fold upregulated), encoding for a chromatin-associated factor involved in cell cycle checkpoint and growth, is correlated with miR-9-3p. GADD45A (1.5-fold upregulated), regulating cell cycle arrest, DNA repair, cell survival, senescence, and apoptosis, is also correlated with miR-9-3p. GPNMB (32-fold downregulated), expressed in a wide array of normal tissues, such as bone, hematopoietic system, and skin, where it influences cell proliferation, adhesion, differentiation, and synthesis of extracellular matrix proteins [93], is targeted by five miRNAs including miR-378a-3p. Among miRNA-correlated genes involved in apoptosis, we identified PDCD4 (proapoptotic, 1.4-fold upregulated) and found out that it is correlated with seven miRNAs, including miR-155-5p and miR-150-3p; BNIP3L (proapoptotic, 1.5-fold downregulated) also correlated with seven miRNAs, including miR-155-5p and miR-9-3p; APAF1 (proapoptotic, 1.3-fold downregulated) correlated with four miRNAs including miR-155-5p and miR-9-3p; and PTEN (proapoptotic) correlated with seven miRNAs including miR-155-5p. Notably, many transcripts (i.e., BCL6, PTEN, BNIP3L, PDCD4, NKX3-1, and GPNMB) are targeted by multiple miRNAs, indicating a pleiotropic effect in gene regulation by coexpressed endogenous miRNAs in MMG. Moreover, our results suggest that under MMG condition a small group of miRNAs regulates transcriptome by modulating the same transcripts within one pathway.

To validate the results of Gene Ontology analysis, we evaluated whether the GO categories “regulation of cell proliferation” and “regulation of programmed cell death” were affected by MMG incubation by performing biological assays of T-cell cloning and apoptosis induction. Our results show that cloning ability of PBLs was lower after 24 h incubation in MMG than in 1 g, in accordance with the suppression of proliferative response of human lymphocytes to mitogenic stimulation in microgravity [94, 95]. The ability to originate clones in PBLs incubated for 48h and 72 h decreased in both gravity conditions probably because the longer G_0 -phase condition experienced by PBLs affected their responsiveness to enter into cell cycle. The antiproliferative effect of microgravity has been recently reported also in human thyroid cancer cells [96] and in human lung adenocarcinoma cells [97]. Our results of apoptosis induction demonstrated that both the formation of apoptotic bodies activation and caspase-3 activation increased significantly in PBLs incubated in MMG than in 1 g. The activation of apoptotic process seems related to the overexpression of PDCD4 and RELA rather than to the underexpression of BNIP3L and APAF1, indicating the existence of complex regulatory networks between miRNAs and mRNAs that occur at different levels of regulation. IFN- γ , besides having an important role in activating innate and adaptive immune responses, plays important roles in

inhibiting cell proliferation and inducing apoptosis. Its overexpression in MMG, mediated by miR-9-3p and miR-155-5p, could thus mediate the antiproliferative effect and the apoptosis induction. In addition, the correlation between miR-9-3p and TP53BP1 could explain the clonogenicity decrease and apoptosis increase in PBLs incubated in MMG. Indeed, overexpression of TP53BP1 has been demonstrated to decrease the clonogenicity and induce apoptosis in ovarian cancer cells [98].

5. Conclusions

Our results show that MMG leads to changes in expression level of a considerable fraction of microRNAome and transcriptome in human PBLs. miRNAs differentially expressed in MMG are correlated with immune/inflammatory-related genes, as IFNG, accordingly with the important role of miRNAs in immune function regulation. Since inflammation works as a tumor-promoting agent, the abnormal expression of such miRNAs under microgravity condition could influence the carcinogenic process by affecting cancer cell immune escape. Moreover, miRNAs mostly dysregulated in MMG, such as miR-9, miR-155, and miR-150, are oncogenic, suggesting that their abnormal expression can influence the carcinogenic process. The results of miRNA-mRNA integration analysis demonstrate that MMG increases the transcriptome plasticity compared with 1g condition and that categories of regulation of cell proliferation and programmed cell death are affected by MMG, as confirmed by *in vitro* experimental validation. Taken together, our results of high-throughput expression analysis and miRNA-mRNA integration analysis give new insight into the complex genetic mechanisms of cell response to stress environment under reduced gravity.

Conflict of Interests

The authors declare that there is no conflict of interests regarding the publication of this paper.

Authors' Contribution

M. Mognato and C. De Pittà conceived and designed the experiments. C. Girardi, S. Casara, and M. Mognato performed the experiments. C. De Pittà, C. Romualdi, E. Calura, L. Celotti, and M. Mognato analyzed the data. M. Mognato and L. Celotti wrote the paper. Cristina Girardi and Cristiano De Pittà contributed equally to this work.

Acknowledgments

The authors gratefully acknowledge M. De Bernard for critical discussion and R. Mazza for graphical support. This work was done with the support of the Italian Space Agency (ASI, XMAB, from Molecules to Man, 1/014/06/0) to L. Celotti and of the University of Padova (CPDA061783) to M. Mognato. The authors also apologize to the authors whose work could not be cited due to space limitations.

References

- [1] R. H. Fitts, D. R. Riley, and J. J. Widrick, "Functional and structural adaptations of skeletal muscle to microgravity," *Journal of Experimental Biology*, vol. 204, no. 18, pp. 3201–3208, 2001.
- [2] M. Narici, B. Kayser, P. Barattini, and P. Cerretelli, "Effects of 17-day spaceflight on electrically evoked torque and cross-sectional area of the human triceps surae," *European Journal of Applied Physiology*, vol. 90, no. 3-4, pp. 275–282, 2003.
- [3] S. Trappe, D. Costill, P. Gallagher et al., "Exercise in space: human skeletal muscle after 6 months aboard the International Space Station," *Journal of Applied Physiology*, vol. 106, no. 4, pp. 1159–1168, 2009.
- [4] S. I. M. Carlsson, M. T. S. Bertilaccio, E. Ballabio, and J. A. M. Maier, "Endothelial stress by gravitational unloading: effects on cell growth and cytoskeletal organization," *Biochimica et Biophysica Acta*, vol. 1642, no. 3, pp. 173–179, 2003.
- [5] M. Infanger, P. Kossmehl, M. Shakibaei et al., "Induction of three-dimensional assembly and increase in apoptosis of human endothelial cells by simulated microgravity: impact of vascular endothelial growth factor," *Apoptosis*, vol. 11, no. 5, pp. 749–764, 2006.
- [6] R. M. Baevesky, V. M. Baranov, I. I. Funtova et al., "Autonomic cardiovascular and respiratory control during prolonged spaceflights aboard the International Space Station," *Journal of Applied Physiology*, vol. 103, no. 1, pp. 156–161, 2007.
- [7] J. D. Sibonga, H. J. Evans, H. G. Sung et al., "Recovery of spaceflight-induced bone loss: bone mineral density after long-duration missions as fitted with an exponential function," *Bone*, vol. 41, no. 6, pp. 973–978, 2007.
- [8] J. H. Keyak, A. K. Koyama, A. LeBlanc, Y. Lu, and T. F. Lang, "Reduction in proximal femoral strength due to long-duration spaceflight," *Bone*, vol. 44, no. 3, pp. 449–453, 2009.
- [9] O. Ullrich, K. Huber, and K. Lang, "Signal transduction in cells of the immune system in microgravity," *Cell Communication and Signaling*, vol. 6, article 9, 2008.
- [10] B. E. Crucian, R. P. Stowe, D. L. Pierson, and C. F. Sams, "Immune system dysregulation following short- vs long-duration spaceflight," *Aviation Space and Environmental Medicine*, vol. 79, no. 9, pp. 835–843, 2008.
- [11] G. Sonnenfeld, J. S. Butel, and W. T. Shearer, "Effects of the space flight environment on the immune system," *Reviews on Environmental Health*, vol. 18, no. 1, pp. 1–17, 2003.
- [12] G. Sonnenfeld, "Editorial: space flight modifies T cell activation—role of microgravity," *Journal of Leukocyte Biology*, vol. 92, no. 6, pp. 1125–1126, 2012.
- [13] A. Semov, N. Semova, C. Lacelle et al., "Alterations in TNF- and IL-related gene expression in space-flown WI38 human fibroblasts," *The FASEB Journal*, vol. 16, no. 8, pp. 899–901, 2002.
- [14] T. T. Chang, I. Walther, C.-F. Li et al., "The Rel/NF- κ B pathway and transcription of immediate early genes in T cell activation are inhibited by microgravity," *Journal of Leukocyte Biology*, vol. 92, no. 6, pp. 1133–1145, 2012.
- [15] M. L. Lewis, L. A. Cubano, B. Zhao et al., "cDNA microarray reveals altered cytoskeletal gene expression in space-flown leukemic T lymphocytes (Jurkat)," *The FASEB Journal*, vol. 15, no. 10, pp. 1783–1785, 2001.
- [16] S. J. Pardo, M. J. Patel, M. C. Sykes et al., "Simulated microgravity using the Random Positioning Machine inhibits differentiation and alters gene expression profiles of 2T3 preosteoblasts," *American Journal of Physiology*, vol. 288, no. 6, pp. C1211–C1221, 2005.

- [17] M. Monticone, Y. Liu, N. Pujic, and R. Cancedda, "Activation of nervous system development genes in bone marrow derived mesenchymal stem cells following spaceflight exposure," *Journal of Cellular Biochemistry*, vol. 111, no. 2, pp. 442–452, 2010.
- [18] D. Grimm, J. Bauer, P. Kossmehl et al., "Simulated microgravity alters differentiation and increases apoptosis in human follicular thyroid carcinoma cells," *The FASEB Journal*, vol. 16, no. 6, pp. 604–606, 2002.
- [19] M. Maccarrone, N. Battista, M. Meloni et al., "Creating conditions similar to those that occur during exposure of cells to microgravity induces apoptosis in human lymphocytes by 5-lipoxygenase-mediated mitochondrial uncoupling and cytochrome c release," *Journal of Leukocyte Biology*, vol. 73, no. 4, pp. 472–481, 2003.
- [20] S. J. Crawford-Young, "Effects of microgravity on cell cytoskeleton and embryogenesis," *International Journal of Developmental Biology*, vol. 50, no. 2-3, pp. 183–191, 2006.
- [21] N. E. Ward, N. R. Pellis, S. A. Risin, and D. Risin, "Gene expression alterations in activated human T-cells induced by modeled microgravity," *Journal of Cellular Biochemistry*, vol. 99, no. 4, pp. 1187–1202, 2006.
- [22] J. Q. Clement, S. M. Lacy, and B. L. Wilson, "Gene expression profiling of human epidermal keratinocytes in simulated microgravity and recovery cultures," *Genomics, Proteomics and Bioinformatics*, vol. 6, no. 1, pp. 8–28, 2008.
- [23] R. Kumari, K. P. Singh, and J. W. DuMond Jr., "Simulated microgravity decreases DNA repair capacity and induces DNA damage in human lymphocytes," *Journal of Cellular Biochemistry*, vol. 107, no. 4, pp. 723–731, 2009.
- [24] C.-Y. Kang, L. Zou, M. Yuan et al., "Impact of simulated microgravity on microvascular endothelial cell apoptosis," *European Journal of Applied Physiology*, vol. 111, no. 9, pp. 2131–2138, 2011.
- [25] J. Krützfeldt, M. N. Poy, and M. Stoffel, "Strategies to determine the biological function of microRNAs," *Nature Genetics*, vol. 38, no. 1, pp. S14–S19, 2006.
- [26] C. A. Nickerson, C. M. Ott, J. W. Wilson et al., "Low-shear modeled microgravity: a global environmental regulatory signal affecting bacterial gene expression, physiology, and pathogenesis," *Journal of Microbiological Methods*, vol. 54, no. 1, pp. 1–11, 2003.
- [27] K. Arunasri, M. Adil, K. Venu Charan, C. Suvro, S. Himabindu Reddy, and S. Shivaji, "Effect of simulated microgravity on *E. coli* K12 MG1655 growth and gene expression," *PLoS ONE*, vol. 8, no. 3, Article ID e57860, 2013.
- [28] O. Marcu, M. P. Lera, M. E. Sanchez et al., "Innate immune responses of *Drosophila melanogaster* are altered by spaceflight," *PLoS ONE*, vol. 6, no. 1, Article ID e15361, 2011.
- [29] Y. Honda, A. Higashibata, Y. Matsunaga et al., "Genes down-regulated in spaceflight are involved in the control of longevity in *Caenorhabditis elegans*," *Scientific Reports*, vol. 2, article 487, 2012.
- [30] A. I. Manzano, J. J. W. A. van Loon, P. C. M. Christianen, J. M. Gonzalez-Rubio, F. J. Medina, and R. Herranz, "Gravitational and magnetic field variations synergize to cause subtle variations in the global transcriptional state of Arabidopsis in vitro callus cultures," *BMC Genomics*, vol. 13, no. 1, article 105, 2012.
- [31] D. P. Bartel, "MicroRNAs: target recognition and regulatory functions," *Cell*, vol. 136, no. 2, pp. 215–233, 2009.
- [32] H. Guo, N. T. Ingolia, J. S. Weissman, and D. P. Bartel, "Mammalian microRNAs predominantly act to decrease target mRNA levels," *Nature*, vol. 466, no. 7308, pp. 835–840, 2010.
- [33] V. Huang, Y. Qin, J. Wang et al., "RNAa is conserved in mammalian cells," *PLoS ONE*, vol. 5, no. 1, Article ID e8848, 2010.
- [34] L. B. Frankel, N. R. Christoffersen, A. Jacobsen, M. Lindow, A. Krogh, and A. H. Lund, "Programmed cell death 4 (PDCD4) is an important functional target of the microRNA miR-21 in breast cancer cells," *The Journal of Biological Chemistry*, vol. 283, no. 2, pp. 1026–1033, 2008.
- [35] M. N. Poy, M. Spranger, and M. Stoffel, "microRNAs and the regulation of glucose and lipid metabolism," *Diabetes, Obesity and Metabolism*, vol. 9, no. 2, pp. 67–73, 2007.
- [36] N. Stern-Ginossar, N. Elefant, A. Zimmermann et al., "Host immune system gene targeting by a viral miRNA," *Science*, vol. 317, no. 5836, pp. 376–381, 2007.
- [37] C. J. Marsit, K. Eddy, and K. T. Kelsey, "MicroRNA responses to cellular stress," *Cancer Research*, vol. 66, no. 22, pp. 10843–10848, 2006.
- [38] P. M. Voorhoeve, C. le Sage, M. Schrier et al., "A genetic screen implicates miRNA-372 and miRNA-373 as oncogenes in testicular germ cell tumors," *Cell*, vol. 124, no. 6, pp. 1169–1181, 2006.
- [39] E. A. C. Wiemer, "The role of microRNAs in cancer: no small matter," *European Journal of Cancer*, vol. 43, no. 10, pp. 1529–1544, 2007.
- [40] W. C. S. Cho, "OncomiRs: the discovery and progress of microRNAs in cancers," *Molecular Cancer*, vol. 6, article 60, 2007.
- [41] S. Mi, J. Lu, M. Sun et al., "MicroRNA expression signatures accurately discriminate acute lymphoblastic leukemia from acute myeloid leukemia," *Proceedings of the National Academy of Sciences of the United States of America*, vol. 104, no. 50, pp. 19971–19976, 2007.
- [42] S. M. Hammond, "MicroRNAs as tumor suppressors," *Nature Genetics*, vol. 39, no. 5, pp. 582–583, 2007.
- [43] A. Bisognin, G. Sales, A. Coppe, S. Bortoluzzi, and C. Romualdi, "MAGIA2: from miRNA and genes expression data integrative analysis to microRNA-transcription factor mixed regulatory circuits (2012 update)," *Nucleic Acids Research*, vol. 40, no. 1, pp. W13–W21, 2012.
- [44] M. Mognato and L. Celotti, "Modeled microgravity affects cell survival and HPRT mutant frequency, but not the expression of DNA repair genes in human lymphocytes irradiated with ionising radiation," *Mutation Research*, vol. 578, no. 1-2, pp. 417–429, 2005.
- [45] B. R. Unsworth and P. I. Lelkes, "Growing tissues in microgravity," *Nature Medicine*, vol. 4, no. 8, pp. 901–907, 1998.
- [46] S.-M. Hou, F. J. Van Dam, F. De Zwart et al., "Validation of the human T-lymphocyte cloning assay—ring test report from the EU concerted action on HPRT mutation (EUCAHM)," *Mutation Research*, vol. 431, no. 2, pp. 211–221, 1999.
- [47] C. Girardi, C. de Pittà, S. Casara et al., "Analysis of miRNA and mRNA expression profiles highlights alterations in ionizing radiation response of human lymphocytes under modeled microgravity," *PLoS ONE*, vol. 7, no. 2, Article ID e31293, 2012.
- [48] H. Wang, R. A. Ach, and B. O. Curry, "Direct and sensitive miRNA profiling from low-input total RNA," *RNA*, vol. 13, no. 1, pp. 151–159, 2007.
- [49] B. M. Bolstad, R. A. Irizarry, M. Åstrand, and T. P. Speed, "A comparison of normalization methods for high density oligonucleotide array data based on variance and bias," *Bioinformatics*, vol. 19, no. 2, pp. 185–193, 2003.

- [50] V. G. Tusher, R. Tibshirani, and G. Chu, "Diagnosis of multiple cancer types by shrunken centroids of gene expression," *Proceedings of the National Academy of Sciences of the United States of America*, vol. 98, pp. 5116–5121, 2001.
- [51] G. Sales, E. Calura, P. Martini, and C. Romualdi, "Graphite web: web tool for gene set analysis exploiting pathway topology," *Nucleic Acids Research*, vol. 41, pp. 89–97, 2013.
- [52] F. Xin, M. Li, C. Balch et al., "Computational analysis of microRNA profiles and their target genes suggests significant involvement in breast cancer antiestrogen resistance," *Bioinformatics*, vol. 25, no. 4, pp. 430–434, 2009.
- [53] H. Wang and W.-H. Li, "Increasing MicroRNA target prediction confidence by the relative R2 method," *Journal of Theoretical Biology*, vol. 259, no. 4, pp. 793–798, 2009.
- [54] D. W. Huang, B. T. Sherman, and R. A. Lempicki, "Systematic and integrative analysis of large gene lists using DAVID bioinformatics resources," *Nature Protocols*, vol. 4, no. 1, pp. 44–57, 2009.
- [55] K. J. Livak and T. D. Schmittgen, "Analysis of relative gene expression data using real-time quantitative PCR and the $2^{-\Delta\Delta C_T}$ method," *Methods*, vol. 25, no. 4, pp. 402–408, 2001.
- [56] R. J. Albertini, K. L. Castle, and W. R. Borchering, "T-cell cloning to detect the mutant 6-thioguanine-resistant lymphocytes present in human peripheral blood," *Proceedings of the National Academy of Sciences of the United States of America*, vol. 79, no. 21 I, pp. 6617–6621, 1982.
- [57] M. Mognato, C. Girardi, S. Fabris, and L. Celotti, "DNA repair in modeled microgravity: double strand break rejoining activity in human lymphocytes irradiated with γ -rays," *Mutation Research*, vol. 663, no. 1-2, pp. 32–39, 2009.
- [58] S. Canova, F. Fiorasi, M. Mognato et al., "Modeled microgravity" affects cell response to ionizing radiation and increases genomic damage," *Radiation Research*, vol. 163, no. 2, pp. 191–199, 2005.
- [59] B. P. Lewis, C. B. Burge, and D. P. Bartel, "Conserved seed pairing, often flanked by adenosines, indicates that thousands of human genes are microRNA targets," *Cell*, vol. 120, no. 1, pp. 15–20, 2005.
- [60] M. S. Cline, M. Smoot, E. Cerami et al., "Integration of biological networks and gene expression data using Cytoscape," *Nature Protocols*, vol. 2, no. 10, pp. 2366–2382, 2007.
- [61] F. Censi, A. Giuliani, P. Bartolini, and G. Calcagnini, "A multi-scale graph theoretical approach to gene regulation networks: a case study in atrial fibrillation," *IEEE Transactions on Biomedical Engineering*, vol. 58, no. 10, pp. 2943–2946, 2011.
- [62] P. Chen, C. Price, Z. Li et al., "miR-9 is an essential oncogenic microRNA specifically overexpressed in mixed lineage leukemia-rearranged leukemia," *Proceedings of the National Academy of Sciences of the United States of America*, vol. 110, no. 28, pp. 11511–11516, 2013.
- [63] G. Pignot, G. Cizeron-Clairac, S. Vacher et al., "MicroRNA expression profile in a large series of bladder tumors: identification of a 3-miRNA signature associated with aggressiveness of muscle-invasive bladder cancer," *International Journal of Cancer*, vol. 132, no. 11, pp. 2479–2491, 2013.
- [64] H. M. Namløs, L. A. Meza-Zepeda, T. Barøy et al., "Modulation of the osteosarcoma expression phenotype by microRNAs," *PLoS ONE*, vol. 7, no. 10, Article ID e48086, 2012.
- [65] P. S. Eis, W. Tam, L. Sun et al., "Accumulation of miR-155 and BIC RNA in human B cell lymphomas," *Proceedings of the National Academy of Sciences of the United States of America*, vol. 102, no. 10, pp. 3627–3632, 2005.
- [66] Y. Pan, M. Meng, G. Zhang, H. Han, and Q. Zhou, "Oncogenic microRNAs in the genesis of leukemia and lymphoma," *Current Pharmaceutical Design*, 2014.
- [67] M. V. Iorio, M. Ferracin, C.-G. Liu et al., "MicroRNA gene expression deregulation in human breast cancer," *Cancer Research*, vol. 65, no. 16, pp. 7065–7070, 2005.
- [68] Z. Lu, Y. Ye, D. Jiao, J. Qiao, S. Cui, and Z. Liu, "MiR-155 and miR-31 are differentially expressed in breast cancer patients and are correlated with the estrogen receptor and progesterone receptor status," *Oncology Letters*, vol. 4, no. 5, pp. 1027–1032, 2012.
- [69] F. Gao, J. Chang, H. Wang, and G. Zhang, "Potential diagnostic value of miR-155 in serum from lung adenocarcinoma patients," *Oncology Reports*, vol. 31, no. 1, pp. 351–357, 2014.
- [70] G. Higgs and F. Slack, "The multiple roles of microRNA-155 in oncogenesis," *Journal of Clinical Bioinformatics*, vol. 3, no. 1, p. 17, 2013.
- [71] H. Fayyad-Kazan, N. Bitar, M. Najjar et al., "Circulating miR-150 and miR-342 in plasma are novel potential biomarkers for acute myeloid leukemia," *Journal of Translational Medicine*, vol. 11, no. 1, article 31, 2013.
- [72] M. Yanlei, P. Zhang, F. Wang et al., "miR-150 as a potential biomarker associated with prognosis and therapeutic outcome in colorectal cancer," *Gut*, vol. 61, no. 10, pp. 1447–1453, 2012.
- [73] N. K. Jacob, J. V. Cooley, T. N. Yee et al., "Identification of Sensitive Serum microRNA Biomarkers for Radiation Biodosimetry," *PLoS ONE*, vol. 8, no. 2, Article ID e57603, 2013.
- [74] G. J. Zhang, H. Zhou, H. X. Xiao, Y. Li, and T. Zhou, "MiR-378 is an independent prognostic factor and inhibits cell growth and invasion in colorectal cancer," *BMC Cancer*, vol. 14, no. 1, p. 109, 2014.
- [75] M. Sand, M. Skrygan, D. Georgas et al., "Microarray analysis of microRNA expression in cutaneous squamous cell carcinoma," *Journal of Dermatological Science*, vol. 68, no. 3, pp. 119–126, 2012.
- [76] S. Hauser, L. M. Wulfken, S. Holdenrieder et al., "Analysis of serum microRNAs (miR-26a-2*, miR-191, miR-337-3p and miR-378) as potential biomarkers in renal cell carcinoma," *Cancer Epidemiology*, vol. 36, no. 4, pp. 391–394, 2012.
- [77] L. S. Mangala, Y. Zhang, Z. He et al., "Effects of simulated microgravity on expression profile of microRNA in human lymphoblastoid cells," *The Journal of Biological Chemistry*, vol. 286, no. 37, pp. 32483–32490, 2011.
- [78] P. Alexiou, M. Maragkakis, G. L. Papadopoulos, M. Reczko, and A. G. Hatzigeorgiou, "Lost in translation: an assessment and perspective for computational microRNA target identification," *Bioinformatics*, vol. 25, no. 23, pp. 3049–3055, 2009.
- [79] J. Nunez-Iglesias, C.-C. Liu, T. E. Morgan, C. E. Finch, and X. J. Zhou, "Joint genome-wide profiling of miRNA and mRNA expression in Alzheimer's disease cortex reveals altered miRNA regulation," *PLoS ONE*, vol. 5, no. 2, Article ID e8898, 2010.
- [80] L. Ma, Y. Huang, W. Zhu et al., "An integrated analysis of miRNA and mRNA expressions in non-small cell lung cancers," *PLoS ONE*, vol. 6, no. 10, Article ID e26502, 2011.
- [81] J. C. Engelmann and R. Spang, "A least angle regression model for the prediction of canonical and non-canonical miRNA-mRNA interactions," *PLoS ONE*, vol. 7, no. 7, Article ID e40634, 2012.
- [82] N. Bossel Ben-Moshe, R. Avraham, M. Kedmi et al., "Context-specific microRNA analysis: identification of functional microRNAs and their mRNA targets," *Nucleic Acids Research*, vol. 40, no. 21, pp. 10614–10627, 2012.

- [83] S. Artmann, K. Jung, A. Bleckmann, and T. Beißbarth, "Detection of simultaneous group effects in microRNA expression and related target gene sets," *PLoS ONE*, vol. 7, no. 6, Article ID e38365, 2012.
- [84] R. N. Germain, "MHC-dependent antigen processing and peptide presentation: providing ligands for T lymphocyte activation," *Cell*, vol. 76, no. 2, pp. 287–299, 1994.
- [85] I. V. Konstantinova, E. N. Antropova, V. I. Legenkov, and V. D. Zazhirey, "Study of the reactivity of blood lymphoid cells in crew members of Soyuz 6, 7 and 8 before and after space flight," *Kosmicheskaya Biologiya i Meditsina*, vol. 7, no. 6, pp. 35–40, 1973 (Russian).
- [86] A. Cogoli and A. Tschopp, "Lymphocyte reactivity during spaceflight," *Immunology Today*, vol. 6, no. 1, pp. 1–4, 1985.
- [87] N. Guéguinou, C. Huin-Schohn, M. Bascove et al., "Could spaceflight-associated immune system weakening preclude the expansion of human presence beyond Earth's orbit?" *Journal of Leukocyte Biology*, vol. 86, no. 5, pp. 1027–1038, 2009.
- [88] Y. O. Nunez, J. M. Truitt, G. Gorini et al., "Positively correlated miRNA-mRNA regulatory networks in mouse frontal cortex during early stages of alcohol dependence," *BMC Genomics*, vol. 14, p. 725, 2013.
- [89] R. P. Sullivan, L. A. Fogel, J. W. Leong et al., "MicroRNA-155 tunes both the threshold and extent of NK cell activation via targeting of multiple signaling pathways," *The Journal of Immunology*, vol. 191, no. 12, pp. 5904–5913, 2013.
- [90] F. Gao, Z.-L. Zhao, W.-T. Zhao et al., "MiR-9 modulates the expression of interferon-regulated genes and MHC class I molecules in human nasopharyngeal carcinoma cells," *Biochemical and Biophysical Research Communications*, vol. 431, no. 3, pp. 610–616, 2013.
- [91] F. Bazzoni, M. Rossato, M. Fabbri et al., "Induction and regulatory function of miR-9 in human monocytes and neutrophils exposed to proinflammatory signals," *Proceedings of the National Academy of Sciences of the United States of America*, vol. 106, no. 13, pp. 5282–5287, 2009.
- [92] S. Thiele, J. Wittmann, H.-M. Jäck, and A. Pahl, "miR-9 enhances IL-2 production in activated human CD4⁺ T cells by repressing Blimp-1," *European Journal of Immunology*, vol. 42, no. 8, pp. 2100–2108, 2012.
- [93] M. Singh, F. Del carpio-Cano, J. Y. Belcher et al., "Functional roles of osteoactivin in normal and disease processes," *Critical Reviews in Eukaryotic Gene Expression*, vol. 20, no. 4, pp. 341–357, 2010.
- [94] M. Cogoli-Greuter, M. A. Meloni, L. Sciola et al., "Movements and interactions of leukocytes in microgravity," *Journal of Biotechnology*, vol. 47, no. 2-3, pp. 279–287, 1996.
- [95] I. Walther, P. Pippia, M. A. Meloni, F. Turrini, F. Mannu, and A. Cogoli, "Simulated microgravity inhibits the genetic expression of interleukin-2 and its receptor in mitogen-activated T lymphocytes," *FEBS Letters*, vol. 436, no. 1, pp. 115–118, 1998.
- [96] X. Ma, J. Pietsch, M. Wehland et al., "Differential gene expression profile and altered cytokine secretion of thyroid cancer cells in space," *The FASEB Journal*, vol. 28, no. 2, pp. 813–835, 2014.
- [97] D. Chang, H. Xu, Y. Guo et al., "Simulated microgravity alters the metastatic potential of a human lung adenocarcinoma cell line," *In Vitro Cellular and Developmental Biology—Animal*, vol. 49, no. 3, pp. 170–177, 2013.
- [98] S. Hong, X. Li, Y. Zhao, Q. Yang, and B. Kong, "53BP1 suppresses tumor growth and promotes susceptibility to apoptosis of ovarian cancer cells through modulation of the Akt pathway," *Oncology Reports*, vol. 27, no. 4, pp. 1251–1257, 2012.